

Curves of Minimax Curvature

C. Yalçın Kaya*

Lyle Noakes[†]

Philip Schrader[‡]

April 22, 2024

Abstract

We consider the problem of finding curves of minimum pointwise-maximum curvature, i.e., curves of minimax curvature, among planar curves of fixed length with prescribed endpoints and tangents at the endpoints. We reformulate the problem in terms of optimal control and use the maximum principle, as well as some geometrical arguments, to produce a classification of the types of solutions. Using the classification, we devise a numerical method which reduces the infinite-dimensional optimization problem to a finite-dimensional problem with just six variables. The solution types, together with some further observations on optimality, are illustrated via numerical examples.

Key words. Minimax curvature, Markov–Dubins path, Optimal control, Singular control, Bang–bang control.

AMS subject classifications. Primary 49J15, 49K15 Secondary 65K10, 90C30

1 Introduction

We are interested in finding a curve $z : [0, t_f] \rightarrow \mathbb{R}^2$ which minimises the almost everywhere (a.e.) pointwise maximum curvature of $z(t)$, i.e. the L^∞ -norm of the curvature, among all curves having fixed length; prescribed endpoints z_0 and z_f at 0 and t_f respectively; and prescribed tangents v_0 and v_f at the endpoints. Since the curvature is independent of parametrisation we will consider only curves which are parametrised with respect to arc length so that the curvature is $\|\ddot{z}(t)\|$, and the parameter t_f is the length of the whole curve (and therefore t_f is fixed). The problem can then be posed as

$$(P) \begin{cases} \min_{z(\cdot)} & \max_{t \in [0, t_f]} \|\ddot{z}(t)\| \\ \text{s.t.} & z(0) = z_0, z(t_f) = z_f, \\ & \dot{z}(0) = v_0, \dot{z}(t_f) = v_f, \\ & \|\dot{z}(t)\| = 1, \text{ for a.e. } t \in [0, t_f], \end{cases}$$

where $\dot{z} = dz/dt$, $\ddot{z} = d^2z/dt^2$, $\|\cdot\|$ is the Euclidean norm, and v_0 and v_f are given such that $\|v_0\| = \|v_f\| = 1$.

*Mathematics, UniSA STEM, University of South Australia, Mawson Lakes, S.A. 5095, Australia. E-mail: yalcin.kaya@unisa.edu.au .

[†]Department of Mathematics and Statistics, The University of Western Australia, Nedlands WA 6009, Australia. Email: Lyle.Noakes@uwa.edu.au .

[‡]School of Mathematics, Statistics, Chemistry and Physics, Murdoch University, Murdoch WA 6150, Australia. Email: Phil.Schrader@murdoch.edu.au

If the L^∞ -norm is replaced by the squared L^2 -norm, of \ddot{z} , namely $\int_0^{t_f} \|\ddot{z}(t)\|^2 dt$, then critical curves for Problem (P) become the celebrated (fixed-length) *Euler's elastica*. The L^p -norm generalizations of the Euler elastica problem for $p \in [1, \infty)$, where $\int_0^{t_f} \|\ddot{z}(t)\|^2 dt$ is replaced by $\int_0^{t_f} \|\ddot{z}(t)\|^p dt$, have been referred to as the p -*elastica* problem in the literature—see [9]. Similarly, potential minimisers of Problem (P) have been called the ∞ -*elastica* in [20]. Here we refer to (P) as the problem of finding *curves of minimum pointwise-maximum curvature*, or simply *curves of minimax curvature*, because it is more descriptive and we are ultimately focused on finding global minimisers.

Another problem related to (P) is the Markov–Dubins problem, in which one is to minimize this time the (free) length t_f of the curve of interest subject to a fixed bound a imposed on the curvature, while the remaining constraints appearing in (P) are kept in place. This problem was first proposed and some instances studied by Andrey Markov in 1889 [17] (also see [16]) but fully solved by Lester Dubins only in 1957 [5]. Dubins' result characterizes minimum-length solutions in terms of concatenations of straight lines and circular arcs: Let a straight line segment be denoted by an S and a circular arc of the maximum allowed curvature a (or, turning radius $1/a$) by a C , then the shortest curve is a concatenation of type CCC , or of type CSC , or a subset thereof. See [10] and the references therein for a literature survey of the Markov–Dubins problem.

The first published work on Problem (P) appears to be that of Moser [20] where it is studied for curves in \mathbb{R}^n , followed by the extension to Riemannian manifolds in [7]. In [20] ∞ -elastica are defined as minimisers of the sum of maximum curvature and a penalty term which is a kind of L^2 -distance between curves. In order to obtain differential equations which characterise ∞ -elastica, Moser studies the Euler–Lagrange equations for the sum of p -elastic energy with the same penalty term, in the limit $p \rightarrow \infty$. From the differential equations Moser obtains a classification of ∞ -elastica as concatenations of circular arcs and straight lines, similar to the solutions of the Markov–Dubins problem, except that ∞ -elastica can contain more than three pieces, and closed loops are allowed. If we denote by O a full circle with the maximum curvature, and C, S as before, the conclusion is that ∞ -elastica can be of type $CSOSOC$, perhaps with more or less loops and straight line segments, or of type $CC\dots C$ with any number of C segments and such that the interior segments have equal length and alternating orientation.

The present work takes a fundamentally different approach to that of Moser: we show that by using the same technique applied in [15], Problem (P) can be reformulated as an optimal control problem without any approximation by p -elastic energy. As usual, the maximum principle then provides us with necessary conditions for optimality in the form of differential equations for the state and costate variables, and constraints on the control. A careful analysis of these conditions – in particular of the phase portrait of the switching function, which is very similar to the analysis of the Markov–Dubins problem in [10, 11] – allows us to draw similar conclusions to Moser's about which types of curves can be optimal.

The necessary conditions obtained from the maximum principle are then combined with a series of geometric arguments, such as Lemma 21 showing that a curve of type $CCCC$ cannot be optimal because it can be deformed into a feasible curve with the same maximum curvature, but which does not satisfy the necessary conditions. These observations lead to our main result, a refined classification in Theorem 22: any solution to Problem (P) is of type CCC , or CSC , or COC , or SOS , or a subset thereof, with all circular arcs having the same maximum possible radius (or minimum possible maximum curvature). So we have that, just like in the Markov–Dubins problem, solutions of problem (P) cannot consist of more than three segments. However, unlike in the Markov–Dubins problem, under specific conditions (Propositions 23 and 25), they can contain closed circular loops.

Since Problem (P) is related to the Markov–Dubins problem by interchange of constraint and cost, it is perhaps not surprising that the solutions are so similar. Indeed, a relationship between

solutions of the two problems was established in [20, Proposition 5]: a solution of the Markov–Dubins problem is a solution to Problem (P). In Theorem 5 we give an alternative proof of this fact in terms of the optimal control formulation, and then demonstrate that the converse does not hold (Remark 6).

We devise a numerical method, which, using the classification of the solution curves stated in Theorem 22 and switching time optimization techniques, reduces the infinite-dimensional optimization problem (P) to a finite-dimensional optimization problem (Ps) with just six variables. We carry out extensive numerical experiments. We especially focus on solutions containing a loop to exemplify the specific results involving loops, as well as gain insights about those instances for which no specific results are available.

The paper is organized as follows. In Section 2, we reformulate Problem (P) as an optimal control problem. In Section 3, we write down the maximum principle for the optimal control problem. In Section 4, we classify the types of solutions for Problem (P) and provide the main theoretical result as Theorem 22. In Section 5, we develop a numerical method for solving Problem (P), and provide example applications and numerical solutions using off-the-shelf optimization software, so as to illustrate the theoretical results. Finally, in Section 6, concluding remarks and possible directions for future work are provided.

2 Reformulations

Obviously, if the distance separating z_0 and z_f is more than the fixed length t_f then Problem (P) has no solution. In fact, with $t_f = \|z_0 - z_f\|$, a feasible solution may still not exist. Consider the points $z_0 = (0, 0)$ and $z_f = (1, 0)$. With $t_f = 1$, unless $v_0 = v_f = (1, 0)$, there exists no feasible curve between z_0 and z_f . Therefore we make the following assumption.

Assumption 1 $t_f > \|z_0 - z_f\|$.

Before reformulating (P) as an optimal control problem and classifying the minimisers, we first address the existence of solutions.

Proposition 2 (*Existence of minimisers.*) *Given initial and final points z_0, z_f and directions v_0, v_f as in Problem (P), there exists a minimiser $z \in W^{2,\infty}((0, t_f), \mathbb{R}^2)$ which is a solution to Problem (P).*

Since the proof of Proposition 2 is somewhat long and does not contribute directly to our main result, we defer it until Section 4.1.

Problem (P) is nonsmooth because of the max operator appearing in its objective functional. On the other hand, Problem (P) can be transformed into a smooth variational problem by using a standard technique from nonlinear programming, in the same way it was also done in [15]:

$$(P1) \begin{cases} \min_{a, z(\cdot)} & a \\ \text{s.t.} & z(0) = z_0, \quad z(t_f) = z_f, \\ & \dot{z}(0) = v_0, \quad \dot{z}(t_f) = v_f, \\ & \|\ddot{z}(t)\| \leq a, \quad \|\dot{z}(t)\| = 1, \text{ for a.e. } t \in [0, t_f], \end{cases}$$

where the bound $a \geq 0$ is a new optimization variable of the problem.

Remark 3 One has the solution $a = 0$ if and only if the curve joining z_0 and z_f is a straight line. This is possible only in the case when $v_0 = v_f$ and v_0 and v_f are colinear with $z_f - z_0$. \square

Problem (P) can equivalently be cast as an optimal control problem as follows. Let $z(t) := (x(t), y(t)) \in \mathbb{R}^2$, with $\dot{x}(t) := \cos \theta(t)$ and $\dot{y}(t) := \sin \theta(t)$, where $\theta(t)$ is the angle the velocity vector $\dot{z}(t)$ of the curve $z(t)$ makes with the horizontal. These definitions verify that $\|\dot{z}(t)\| = 1$. Moreover,

$$\|\ddot{z}\|^2 = \ddot{x}^2 + \ddot{y}^2 = \dot{\theta}^2.$$

Therefore, $|\dot{\theta}(t)|$ is nothing but the curvature. In fact, $\dot{\theta}(t)$ itself, which can be positive or negative, is referred to as the *signed curvature*. For example, consider a vehicle travelling along a circular path. If $\dot{\theta}(t) > 0$ then the vehicle travels in the counter-clockwise direction, i.e., it *turns left*, and if $\dot{\theta}(t) < 0$ then the vehicle travels in the clockwise direction, i.e., it *turns right*. If $\dot{\theta}(t) = 0$ then the vehicle travels along a straight line.

Suppose that the directions at the points z_0 and z_f are denoted by the angles θ_0 and θ_f , respectively. The curvature minimizing problem (P1), or equivalently Problem (P), can then be re-written as a (*parametric*) *optimal control problem*, where the objective functional is the maximum curvature a (the *parameter*), and x , y and θ are the *state variables* and u is the *control variable*:

$$(Pc) \begin{cases} \min_{a, u(\cdot)} a \\ \text{s.t. } \dot{x}(t) = \cos \theta(t), \quad x(0) = x_0, \quad x(t_f) = x_f, \\ \dot{y}(t) = \sin \theta(t), \quad y(0) = y_0, \quad y(t_f) = y_f, \\ \dot{\theta}(t) = u(t), \quad \theta(0) = \theta_0, \quad \theta(t_f) = \theta_f, \\ |u(t)| \leq a, \quad \text{for a.e. } t \in [0, t_f]. \end{cases}$$

Recall by Remark 3 that the solution to Problem (P), equivalently (Pc), with $a = 0$ constitutes a special configuration of the given oriented endpoints: the angle $\theta(t) = \theta_0 = \theta_f = \arctan((y_f - y_0)/(x_f - x_0))$ for all $t \in [0, t_f]$, and so the curve $z(t)$ is a straight line from (x_0, y_0) to (x_f, y_f) .

Note that with the unit speed constraint $\|\dot{z}(t)\| = 1$ in Problem (P) the solution curve $z(t)$ is parametrized with respect to its length. Therefore the terminal time t_f is nothing but the length of the curve $z(t)$. When the maximum allowed curvature a is fixed, the length t_f is allowed to vary, and the objective functional a in Problem (Pc) is replaced by t_f , Problem (Pc) becomes the celebrated Markov–Dubins problem [5, 16, 17], where one looks for the shortest curve between the oriented points (x_0, y_0, θ_0) and (x_f, y_f, θ_f) , with a prescribed bound a on its curvature:

$$(MD) \begin{cases} \min_{t_f, u(\cdot)} t_f \\ \text{s.t. } \text{Constraints in Problem (Pc) with } a \text{ fixed.} \end{cases}$$

Let a straight line segment be denoted by an S and a circular arc segment of curvature a (or, turning radius $1/a$) by a C . Dubins' result is stated in terms of concatenations of type S and type C curve segments in the following theorem.

Theorem 4 (Dubins' theorem [5]) *A solution to Problem (MD) exists, and any such solution, that is to say, any C^1 and piecewise- C^2 curve of minimum length in the plane between two prescribed endpoints, where the slopes of the curve at these endpoints as well as a bound on the pointwise curvature are also prescribed, is of type CSC, or of type CCC, or a subset thereof.*

In the following theorem, we establish a relationship between Problems (MD) and (Pc). In fact, the proof of the theorem utilizes Theorem 4 as well as the following simple observation: Problem (MD) minimizes the length t_f while the bound a on the curvature is fixed, and Problem (Pc) minimizes a while t_f is kept fixed.

Theorem 5 (Solutions of (MD) and (Pc)) Any solution t_f^* to Problem (MD) with $a = a^*$ fixed is the solution a^* to Problem (Pc) with $t_f = t_f^*$ fixed.

Proof. Suppose that, with $a = a^*$ fixed, the solution of Problem (MD) yields t_f^* . By Theorem 4, either $|\dot{\theta}^*(t)| = a^*$ or $\dot{\theta}^*(t) = 0$, a.e. $t \in [0, t_f^*]$; in other words, with the optimal length t_f^* , the optimal angular velocity $\dot{\theta}^*$ has to satisfy

$$|\dot{\theta}^*(t)| \notin (0, a^*), \quad \text{a.e. } t \in [0, t_f^*]. \quad (1)$$

Now suppose that, with $t_f = t_f^*$ fixed, solution of Problem (Pc) yields \hat{a} . Obviously, $0 \leq \hat{a} \leq a^*$. We can obtain a contradiction for the case when $\hat{a} < a^*$ as follows.

- (i) $\hat{a} \neq 0$: Since this solution of Problem (Pc) satisfies the constraints of Problem (MD) with $a = a^*$, and has the optimal length t_f^* for Problem (MD), it must also be a solution of (MD). Then it must satisfy (1). However, since it is a solution of Problem (Pc) it also satisfies $0 \leq |\dot{\theta}(t)| \leq \hat{a}$ for a.e. $t \in [0, t_f^*]$, and so we cannot have $\hat{a} < a^*$ unless $\hat{a} = 0$.
- (ii) $\hat{a} = 0$: In this case, we have the trivial case $\theta_0 = \theta_f = \arctan((y_f - y_0)/(x_f - x_0))$, which yields $\dot{\theta}(t) = 0$, a.e. $t \in [0, t_f^*]$, as the solution of both Problems (Pc) and (MD), with $\hat{a} = a^* = 0$.

Therefore, with $t_f = t_f^*$ fixed, the solution of Problem (Pc) yields $\hat{a} = a^*$. So, if the pair (t_f^*, a^*) solves Problem (MD), then it also solves Problem (Pc). \square

Remark 6 The converse of Theorem 5 is not true: Consider the oriented points $(x_0, y_0, \theta_0) = (0, 0, 0)$ and $(x_f, y_f, \theta_f) = (1, 0, 0)$. Fix $t_f = \hat{t}_f = 2 > \|x_f - x_0\| = 1$. Then clearly the solution \hat{a} to Problem (Pc) is bounded away from 0, as $\hat{a} = 0$ is the solution where x_0 and x_f are joined by a straight line with $t_f = 1 < 2$. On the other hand, with the curvature bound $a = \hat{a}$ fixed, Problem (MD) yields the solution $t_f^* = 1$, and $\dot{\theta}^*(t) = 0$ for all $t \in [0, t_f^*]$ (the straight line joining x_0 and x_f). So one gets $t_f^* < \hat{t}_f$, furnishing a counterexample for the converse of Theorem 5. \square

3 Maximum Principle

In this section, we study the optimality conditions for a re-formulation of Problem (Pc) in a classical form. Let us redefine the control variable u such that $\alpha(t)v(t) := \dot{\theta}(t)$, where $\alpha(t) := a$ and so $\dot{\alpha}(t) := 0$, for a.e. $t \in [0, t_f]$. Problem (Pc), or equivalently Problem (P), can then be re-written as the following *optimal control problem*:

$$(OC) \left\{ \begin{array}{l} \min_{v(\cdot)} \int_0^{t_f} \alpha(t) dt \\ \text{s.t. } \dot{x}(t) = \cos \theta(t), \quad x(0) = x_0, \quad x(t_f) = x_f, \\ \dot{y}(t) = \sin \theta(t), \quad y(0) = y_0, \quad y(t_f) = y_f, \\ \dot{\theta}(t) = \alpha(t)v(t), \quad \theta(0) = \theta_0, \quad \theta(t_f) = \theta_f, \quad |v(t)| \leq 1, \quad \text{for a.e. } t \in [0, t_f], \\ \dot{\alpha}(t) = 0, \quad \text{for a.e. } t \in [0, t_f]. \end{array} \right.$$

Define the *Hamiltonian function* for Problem (OC) as

$$H(x, y, \theta, \alpha, \lambda_0, \lambda_1, \lambda_2, \lambda_3, \lambda_4, v) := \lambda_0 \alpha + \lambda_1 \cos \theta + \lambda_2 \sin \theta + \lambda_3 \alpha v + \lambda_4 \cdot 0, \quad (2)$$

where $\lambda_0 \geq 0$ is a scalar (multiplier) parameter and $\lambda_i : [0, t_f] \rightarrow \mathbb{R}$, $i = 1, 2, 3, 4$, are the *adjoint* (or *costate*) variables. Let

$$H[t] := H(x(t), y(t), \theta(t), \alpha(t), \lambda_0, \lambda_1(t), \lambda_2(t), \lambda_3(t), \lambda_4(t), v(t)).$$

The adjoint variables are required to satisfy

$$\dot{\lambda}_1(t) := -H_x[t] = 0, \quad (3)$$

$$\dot{\lambda}_2(t) := -H_y[t] = 0, \quad (4)$$

$$\dot{\lambda}_3(t) := -H_\theta[t] = \lambda_1(t) \sin \theta(t) - \lambda_2(t) \cos \theta(t), \quad (5)$$

$$\dot{\lambda}_4(t) := -H_\alpha[t] = -\lambda_0 - \lambda_3(t) v(t), \quad \lambda_4(0) = 0, \quad \lambda_4(t_f) = 0, \quad (6)$$

where $H_x = \partial H / \partial x$, etc. By these definitions, the state and adjoint variables verify a Hamiltonian system in that, in addition to (3)–(6), one has $\dot{x}(t) = H_{\lambda_1}[t]$, $\dot{y}(t) = H_{\lambda_2}[t]$, $\dot{\theta}(t) = H_{\lambda_3}[t]$ and $\dot{\alpha}(t) = H_{\lambda_4}[t]$.

Note that (3)–(4) imply that $\lambda_1(t) = \bar{\lambda}_1$ and $\lambda_2(t) = \bar{\lambda}_2$ for all $t \in [0, t_f]$, where $\bar{\lambda}_1$ and $\bar{\lambda}_2$ are constants. Define new constants

$$\rho := \sqrt{\bar{\lambda}_1^2 + \bar{\lambda}_2^2}, \quad \tan \phi := \frac{\bar{\lambda}_2}{\bar{\lambda}_1}. \quad (7)$$

Then (2) and (5) can respectively be re-written as

$$H[t] = a \lambda_0 + \rho \cos(\theta(t) - \phi) + a \lambda_3(t) v(t), \quad (8)$$

where we have also used $\alpha(t) = a$, for all $t \in [0, t_f]$, and

$$\dot{\lambda}_3(t) = \rho \sin(\theta(t) - \phi). \quad (9)$$

Since H does not depend on t explicitly,

$$H[t] = h, \quad (10)$$

where h is some real constant.

The maximum principle [21, Theorem 1] for Problem (OC) can simply be stated as follows. Suppose that $x, y, \theta, \alpha \in W^{1,\infty}(0, t_f; \mathbb{R})$ and $v \in L^\infty(0, t_f; \mathbb{R})$ solve Problem (OC). Then there exist a number $\lambda_0 \geq 0$ and functions $\lambda_i \in W^{1,\infty}(0, t_f; \mathbb{R})$, $i = 1, 2, 3, 4$, such that $\lambda(t) := (\lambda_0, \lambda_1(t), \lambda_2(t), \lambda_3(t), \lambda_4(t)) \neq \mathbf{0}$, for every $t \in [0, t_f]$, and, in addition to the state differential equations and other constraints given in Problem (OC) and the adjoint differential equations (3)–(4), (6) and (9), the following condition holds:

$$u(t) \in \operatorname{argmin}_{|w| \leq 1} H(x(t), y(t), \theta(t), \alpha(t), \lambda_0, \lambda_1(t), \lambda_2(t), \lambda_3(t), \lambda_4(t), w), \quad (11)$$

Using the definition in (2), (11) can be concisely written as

$$v(t) \in \operatorname{argmin}_{|w| \leq 1} a \lambda_3(t) w, \quad (12)$$

which yields the optimal control as

$$v(t) = \begin{cases} 1, & \text{if } a \lambda_3(t) < 0, \\ -1, & \text{if } a \lambda_3(t) > 0, \\ \text{undetermined,} & \text{if } a \lambda_3(t) = 0. \end{cases} \quad (13)$$

Furthermore, (8) and (10) give

$$a \lambda_3(t) v(t) + \rho \cos(\theta(t) - \phi) + a \lambda_0 =: h. \quad (14)$$

The control $v(t)$ to be chosen for the case when $a \lambda_3(t) = 0$ for a.e. $t \in [\zeta_1, \zeta_2] \subset [0, t_f]$ is referred to as *singular control*, because (12) does not yield any further information. On the other hand, when $a \lambda_3(t) \neq 0$ for a.e. $t \in [0, t_f]$ (which implies that $a > 0$), i.e., it is possible to have $\lambda_3(t) = 0$ only for isolated values of t , the control $v(t)$ is said to be *nonsingular*. It should be noted that, if $\lambda_3(\tau) = 0$ only at an isolated point τ , the optimal control at this isolated point can be chosen as $v(\tau) = -1$ or $v(\tau) = 1$, conveniently. Therefore, if the control $v(t)$ is nonsingular, it will take on either the value -1 or 1 , the bounds on the control variable. In this case, the control $v(t)$ is referred to as *bang–bang*. Since the sign of $\lambda_3(t)$ determines the value of the optimal control $v(t)$, λ_3 is referred to as the *switching function*.

Lemma 7 (Singularity and Straight Line Segments) *Suppose that the optimal control $v(t)$ for Problem (OC) is singular over an interval $[\zeta_1, \zeta_2] \subset [0, t_f]$. Then $\theta(t)$ is constant for all $t \in [\zeta_1, \zeta_2]$. Moreover, if $a > 0$ then $v(t) = 0$ for all $t \in [\zeta_1, \zeta_2]$.*

Proof. Suppose that the optimal control $v(t)$ is singular, i.e., $a \lambda_3(t) = 0$, for a.e. $t \in [\zeta_1, \zeta_2] \subset [0, t_f]$. If $a = 0$, then $\dot{\theta}(t) = 0$ and so $\theta(t)$ is constant. If $a > 0$ then $\dot{\lambda}_3(t) = 0$ for a.e. $t \in [\zeta_1, \zeta_2] \subset [0, t_f]$. In other words, from (9), $\sin(\theta(t) - \phi) = 0$, which implies that $\theta(t)$ is constant, i.e., $\theta(t) = u(t) = 0$, for all $t \in [\zeta_1, \zeta_2]$. \square

Remark 8 Using Lemma 7, for $a > 0$, we can rewrite the optimal control in (13) as

$$v(t) = -\operatorname{sgn}(\lambda_3(t)), \quad \text{a.e. } t \in [0, t_f]. \quad (15)$$

When $a \lambda_3(t) = 0$ over an interval of time, $\theta(t)$ is constant, so the solution curve in that interval is a straight line. When $a \lambda_3(t) \neq 0$, i.e., $\lambda_3(t) \neq 0$, over an interval of time the solution curve in that interval is a circular arc segment with radius $1/a$. \square

By Lemma 7, we have established that the only straight-line solution of Problem (OC) is a singular control solution. In the rest of this section we will assume that $a > 0$, as there is nothing more to say for the simple case of $a = 0$, as far as the maximum principle is concerned.

Assumption 9 $a > 0$.

The problems that yield a solution with $\lambda_0 = 0$ are referred to as *abnormal*, so are their solutions, in the optimal control theory literature, for which the conditions obtained from the maximum principle are independent of the objective functional $\int_0^{t_f} \alpha(t) dt$ in Problem (OC) and therefore not sufficiently informative. The problems that yield $\lambda_0 > 0$, and their solutions, are referred to as *normal*. Lemma 10 below states that we can rule out abnormality for Problem (OC).

Lemma 10 (Normality of Solutions) *Problem (OC) is normal, i.e., one can set $\lambda_0 := 1$.*

Proof. For contradiction purposes, suppose that $\lambda_0 = 0$ and recall the assumption that $a > 0$. Then, from (6) and (15), $\dot{\lambda}_4(t) = |\lambda_3(t)| \geq 0$, for every $t \in [0, t_f]$, which, along with the boundary conditions $\lambda_4(0) = \lambda_4(t_f) = 0$, implies that $\lambda_4(t) = \lambda_3(t) = 0$ for every $t \in [0, t_f]$, giving rise to a totally singular solution. This in turn implies that $v(t) = 0$ and so $\dot{\theta}(t) = 0$, for every $t \in [0, t_f]$, and thus $a = 0$, which is a contradiction. Therefore $\lambda_0 > 0$. Then, without loss of generality, one can set $\lambda_0 = 1$. \square

Remark 11 We recall that as proved in [10] a solution to a similar optimal control reformulation of the Markov–Dubins problem (MD) can be abnormal, while we prove in Lemma 10 that there are no abnormal solutions to Problem (OC). \square

Lemma 12 (Singularity and ρ) *Suppose that the optimal control $v(t)$ for Problem (OC) is singular over an interval $[\zeta_1, \zeta_2] \subset [0, t_f]$. Then $\rho = |a - h| \neq 0$, with h as defined in (14).*

Proof. Suppose the optimal control $u(t)$ is singular over $[\zeta_1, \zeta_2] \subset [0, t_f]$. Then $\lambda_3(t) = \dot{\lambda}_3(t) = 0$ for a.e. $t \in [\zeta_1, \zeta_2]$. From (9), $\sin(\theta(t) - \phi) = 0$, which implies that $\cos(\theta(t) - \phi) = 1$ or -1 . Then, substituting $\lambda_3(t) = 0$, $\cos(\theta(t) - \phi) = \pm 1$, and (from Lemma 10) $\lambda_0 = 1$, into (14), one gets $\rho = \mp(a - h) \geq 0$.

Next we show that $\rho \neq 0$. For contradiction purposes, suppose that $\rho = 0$, i.e., $\lambda_1(t) = \lambda_2(t) = 0$, for every $t \in [0, t_f]$, and recall the assumption that $a > 0$. Then $\dot{\lambda}_3(t) = 0$ and so $\lambda_3(t) = 0$, for every $t \in [0, t_f]$. Now from (6), we get $\dot{\lambda}_4(t) = -1$, for every $t \in [0, t_f]$, which does not have a solution with $\lambda_4(0) = \lambda_4(t_f) = 0$. \square

Lemma 13 *The adjoint variable λ_3 for Problem (OC) solves the differential equation*

$$\dot{\lambda}_3^2(t) + (a |\lambda_3(t)| - a + h)^2 = \rho^2. \quad (16)$$

Proof. From (9),

$$\dot{\lambda}_3^2(t) = \rho^2 \sin^2(\theta(t) - \phi) = \rho^2 - \rho^2 \cos^2(\theta(t) - \phi). \quad (17)$$

Using $v(t) = -\text{sgn}(\lambda_3(t))$ and $\lambda_0 = 1$ in (14), one gets

$$\rho \cos(\theta(t) - \phi) = a |\lambda_3(t)| - a + h.$$

Substituting this into the right-hand side of (17) and rearranging give (16). \square

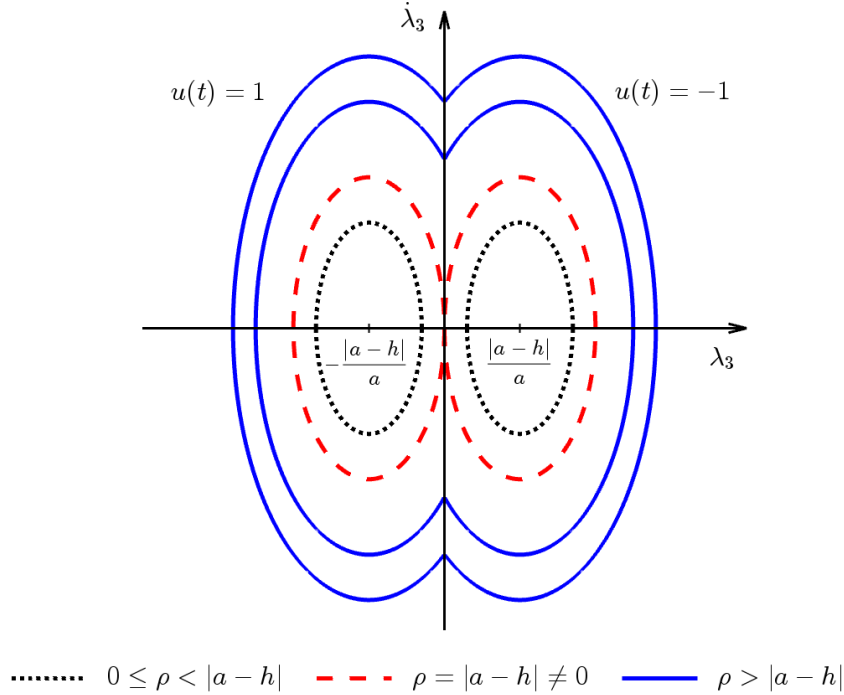
In the rest of the paper, we will at times not show dependence of variables on t for clarity of presentation.

Remark 14 (Phase Portrait for Switchings) Note that the differential equation (16) is given in terms of the *phase variables* λ_3 and $\dot{\lambda}_3$, and can be put into the form

$$\left(\lambda_3 \pm \frac{|a - h|}{a} \right)^2 + \frac{\dot{\lambda}_3^2}{a^2} = \frac{\rho^2}{a^2}, \quad (18)$$

where the “+” sign in the first square term stands for the case when $\lambda_3 < 0$ and the “−” sign for $\lambda_3 > 0$. Equation (18) clearly tells us that the trajectories in the *phase plane* for λ_3 (the $\lambda_3 \dot{\lambda}_3$ -plane) will be pieces or concatenations of pieces of concentric ellipses centred at $(-|a - h|/a, 0)$ for $v(t) = 1$ and $(|a - h|/a, 0)$ for $v(t) = -1$, as shown in Figure 1. Based on the *phase plane diagram*, also referred to as the *phase portrait*, of λ_3 depicted in Figure 1, the following observations are made.

- (i) When $\rho > |a - h|$ the trajectories are concatenations of (pieces of) ellipses, examples of which are shown by (dark blue) solid curves in Figure 1. The ellipses are concatenated at the switching points $(0, \sqrt{\rho^2 - (a - h)^2})$ and $(0, -\sqrt{\rho^2 - (a - h)^2})$, where the value of the bang–bang control $v(t)$ switches from 1 to -1 or from -1 to 1, respectively. The concatenated ellipses cross the λ_3 -axis at two points, $(-(\rho + |a - h|)/a, 0)$ and $((\rho + |a - h|)/a, 0)$. One can promptly deduce from the diagram that if the bang–bang control has two switchings, the second arc must have a length t_f strictly greater than π/a , in other words, the smallest possible curvature a is π/t_f . The diagram, however, does not tell as to how many switchings the optimal control must have.

Figure 1: Phase portrait of (16) for the switching function λ_3 .

- (ii) Recall, by Lemma 12, that $\rho = |a - h| \neq 0$ for singular control. The case when only a part of the trajectory is singular, i.e., *partially singular*, referred to as a *bang-singular* trajectory, is represented by the two unique (red) dashed elliptic curves in Figure 1. Note that singular control takes place only at the origin $(0, 0)$ of the phase plane, with $v(t) = 0$. At any other point, the control trajectory is of bang-bang type. We also note that a trajectory is *totally singular* if, and only if, $a = 0$, the solution given in Remark 3.
- (iii) For the case when $0 \leq \rho < |a - h|$, example elliptic trajectories are shown with (black) dotted curves in Figure 1. The trajectories cross the λ_3 -axis at four distinct points $(-(|a - h| + \rho)/a, 0)$ and $(-(|a - h| - \rho)/a, 0)$ when $\lambda_3 < 0$, and $((|a - h| + \rho)/a, 0)$ and $((|a - h| - \rho)/a, 0)$ when $\lambda_3 > 0$. However, the trajectories no longer intercept the λ_3 -axis; therefore they represent bang-bang control with no switchings, i.e., either $v(t) = 1$ for all $t \in [0, t_f]$ or $v(t) = -1$ for all $t \in [0, t_f]$.

An optimal path will in general be a concatenation of straight lines (i.e., singular arcs, where $v(t) = 0$) and circular arcs (i.e., nonsingular arcs, where $v(t) = 1$ or -1). \square

Lemma 15 *Suppose that optimal control $v(t)$ for Problem (OC) is nonsingular over an interval $[\zeta_3, \zeta_4] \subset [0, t_f]$. Then*

$$|\lambda_3(t)| = \frac{1}{a} [\rho \cos(\theta(t) - \phi) + a - h], \quad \text{for a.e. } t \in [\zeta_3, \zeta_4] \subset [0, t_f]. \quad (19)$$

Proof. Substitution of $v(t) = -\text{sgn}(\lambda_3(t))$ and $\lambda_0 = 1$ into (14) and re-arranging yield the required expression. \square

Lemma 16 (Nonsingular Curves) *Consider Problem (OC) and the maximum principle for it.*

- (a) *If $\rho = 0$, then either $v(t) = 1$ or $v(t) = -1$, for all $t \in [0, t_f]$.*

(b) If $0 < \rho \neq |a - h|$, then $v(t)$ is of bang–bang type.

Proof. (a) Suppose that $\rho = 0$. Then, from Lemma 15, $|\lambda_3(t)| = (a - h)/a$, $\lambda_3(t)$ is a nonzero constant, i.e., $v(t)$ is either 1 or -1 , for all $t \in [0, t_f]$.

(b) Suppose that $0 < \rho \neq |a - h|$. Then, the contrapositive of Lemma 12 states that the optimal control is not singular, i.e., bang–bang. \square

Remark 17 The constant optimal control in Lemma 16(a), $v(t) = 1$ or $v(t) = -1$, and the associated $|\lambda_3(t)| = (a - h)/a$, can be viewed graphically as the limiting case when $\rho \rightarrow 0$ in Figure 1, i.e., the “size” of the black-dotted ellipse shrinks down to zero. \square

4 Classification of Optimal Paths

Denote a straight line segment by S and a circular arc by C , so that a trajectory satisfying the necessary conditions can be described as being of type C, S, CSC, \dots etc. In [10, Lemma 6] the analog of Figure 1 is used to conclude that an optimal path for (MD) contains a straight line segment S then it must be of type CSC, CS, SC , or S . Part of the argument is that a trajectory containing e.g. SCS must traverse a full circle and is therefore not optimal because the objective in the Markov–Dubins problem is to minimize length.

For Problem (OC) we can also conclude from Figure 1 and (9) that SCS must traverse a full circle, but it is no longer obvious that such a path cannot be optimal. In fact we will show that in some cases it *is* optimal (Proposition 23, Proposition 25) while in others it is not (Corollary 20). It will be helpful to introduce the notation O to represent a full circle once covered, and reserve C for circular arcs which are not closed.

Lemma 18 *If $\mathbf{x}^*(t) := (x^*(t), y^*(t), \theta^*(t))$ with $\alpha^*(t) = a^*$ is an optimal path for Problem (OC) then any sub-path of \mathbf{x}^* is also optimal for the inherited constraints. That is, for any $[t_1, t_2] \subset [0, t_f]$ the restriction $\mathbf{x}^*|_{[t_1, t_2]}$ is optimal for problem (OC) with the constraints replaced by $x(t_i) = x^*(t_i)$, $y(t_i) = y^*(t_i)$, $\theta(t_i) = \theta^*(t_i)$ for $i = 1, 2$, with $t \in [t_1, t_2]$.*

Proof. If the sub-path is a line then it is optimal. Assume it is not a line, and suppose it is not optimal. Then there exists a path satisfying the inherited constraints and having $0 < a < a^*$, meaning it contains circular arcs with lower curvature than those in \mathbf{x}^* . We can insert it between $\mathbf{x}^*([0, t_1])$ and $\mathbf{x}^*([t_2, t_f])$ to obtain a new path $\tilde{\mathbf{x}}(t)$. Now either \mathbf{x}^* and $\tilde{\mathbf{x}}$ have the same maximum curvature, or the maximum curvature of $\tilde{\mathbf{x}}$ is smaller. The latter contradicts our assumption that \mathbf{x}^* is optimal. If they have the same maximum curvature, then $\tilde{\mathbf{x}}$ contains at least one circular arc with curvature a^* and at least one circular arc with curvature a , and so it does not satisfy the necessary conditions for optimality (specifically (13)). It then follows that a^* cannot be a minimum, again contradicting our assumption on \mathbf{x} . \square

Lemma 19 *Any path of type XCY , where X, Y are C, O or S but not both C , is not optimal.*

Proof. Since at least one of X and Y is S or O , in order for the path to be optimal it must have switching function on the (red) dashed ellipses in Figure 1. But since the middle C in XCY does not traverse a full loop it is impossible for the switching function to traverse a full ellipse and switch to S or to C or O with the opposite orientation. (Note that we are assuming that, for example, in CCS the two arcs have opposite orientation, otherwise this path would be written as CS or OCS). In the case of CCO (similarly OCC) this is perhaps not immediately obvious because the middle

C and the O may have the same orientation, and then the switching function would not need to return to the origin of the phase portrait in Figure 1. However, we can reflect the loop about the endpoint with no change in maximum curvature, and the resulting path again is not compatible with the necessary conditions on the switching function. \square

Corollary 20 *Any path of type $SOSC$ or any permutation thereof, or type $COCC$ or any permutation thereof, cannot be optimal.*

Proof. Note that the loop can be shifted anywhere along the path without changing the maximum curvature. For example a path of type $SOSC$ has the same maximum curvature as the path of type SCO obtained by shifting the loop to the end. The latter is not optimal by Lemma 19, and therefore neither is the former. Similarly, the other permutations of $SOSC$ and permutations of $COCC$ are not optimal. \square

Lemma 21 *A $CCCC$ trajectory is not a solution to (Pc).*

Sketch of the proof. Following the observations in Remark 14, a $CCCC$ trajectory must be of the type pictured in Figure 2, with the second and third circular arcs having the same length, which is greater than π/a . The idea behind this proof is very simple: beginning with the $CCCC$ trajectory, we roll the circle c_1 around the circle c_0 while allowing the third arc to be ‘pulled-tight’ and allowing the fourth arc to relax to the circle centred at \tilde{c}_2 , to obtain the dashed trajectory in Figure 2. This new trajectory doesn’t satisfy the necessary conditions for optimality because the second circular arc doesn’t traverse a full circle (see Remark 14). However, it has the same maximum curvature as the $CCCC$ trajectory we started with, and therefore this maximum curvature cannot be minimal.

The reason the proof becomes somewhat technical below is that it does not seem to be easy to solve explicitly for the rolling angle β_0 which ensures that the dashed curve satisfies the length constraint. Instead we will prove (taking care with a couple of slightly different cases) that the length depends continuously on β_0 , and that there exist values of β_0 such that the length is greater than and less than the length of the original $CCCC$ trajectory.

Proof.

Referring to Figure 2, we consider the points c_i to be in the complex plane with $c_0 = 0$, and assume that the radius of each of the circles is 1.

Case 1a: $\alpha_3 < \pi/2$ and $\gamma < \pi/2$. We reflect c_3 across θ_f and rotate c_1 about c_0 until we obtain the $CCSC$ trajectory pictured in Figure 2. Supposing there exists β_0 such that the pictured trajectory satisfies our length constraint, then it satisfies all the constraints of Problem (Pc). As explained in the sketch above, this second trajectory has the same maximum curvature as the original $CCCC$ but cannot be optimal, and therefore the $CCCC$ trajectory is not optimal.

It remains to prove that there exists β_0 such that the $CCSC$ trajectory satisfies the length constraint. Referring to Figure 2 we have

$$\begin{aligned}\tilde{c}_1 &= 2e^{i\beta_0} \\ \tilde{c}_2 &= z_f + e^{i(\pi/2+\theta_f)} \\ L &= \alpha_0 + \beta_0 + \beta_1 + \ell + \beta_2 \\ \beta_0 - \beta_1 + \beta_2 &= \theta_f - \pi/2\end{aligned}$$

where L is the total length. If we let

$$w = \tilde{c}_2 - \tilde{c}_1 = z_f + e^{i(\pi/2+\theta_f)} - 2e^{i\beta_0}$$

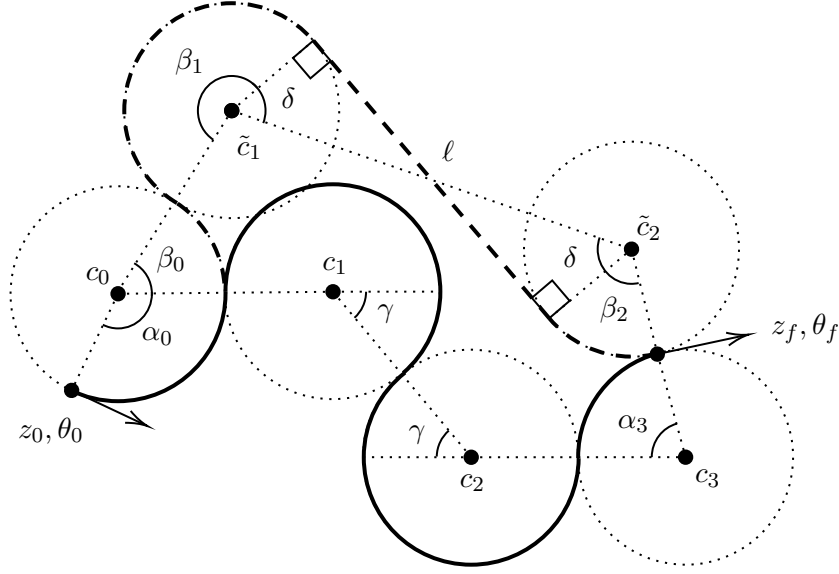


Figure 2: Diagram for the proof of Lemma 21, case 1: trajectory of type $CCCC$ (solid) which satisfies the necessary conditions from the maximum principle, and another of type $CCSC$ (dashed) with the same maximum curvature which does not.

then

$$\begin{aligned}
\ell &= \sqrt{|w|^2 - 2} \\
\delta &= \cos^{-1}(2/|w|) \\
\beta_1 &= \delta - \arg(w) - \pi - \beta_0 = \cos^{-1}(2/|w|) - \arg(w) - \pi - \beta_0 \\
\beta_2 &= \theta_f - \pi/2 + \beta_1 - \beta_0 = \theta_f - 3\pi/2 + \cos^{-1}(2/|w|) - \arg(w) - 2\beta_0 \\
L &= \alpha_0 + 2\beta_1 + \ell + \theta_f - \pi/2 = \alpha_0 + 2\cos^{-1}(2/|w|) - 2\arg(w) - 2\pi - 2\beta_0 + \ell + \theta_f - \pi/2 \quad (20)
\end{aligned}$$

Since w is determined by the boundary conditions and β_0 , it follows that each of $\ell, \delta, \beta_1, \beta_2$ are determined by the the boundary conditions and β_0 and in fact L depends continuously on β_0 . If we can prove that there are values of β_0 for which L is above and below the length constraint, then by the intermediate value theorem a trajectory satisfying the length constraint exists.

Note that we can make L as large as we like by increasing β_0 , and wrapping the trajectory around the circle centred at c_0 if necessary. To prove that $L < t_f$ can be achieved we consider two cases. First we assume that as in Figure 2 the reflected circle centred at \tilde{c}_2 does not intersect the circle centred at c_1 , and so we can take $\beta_0 = 0$ and observe that the new $CCSC$ trajectory, where the S is a common tangent to c_1 and \tilde{c}_2 , is shorter. In the case where the reflected circle does intersect the circle centred at c_1 , we consider the CCC trajectory pictured in Figure 3. Here $\ell = 0$ and β_0 is at its minimum.

The length of the original trajectory is $L_1 = \alpha_0 + 2\pi + 2\gamma + \alpha_3$, and from (20) the length of the CCC trajectory is $L_2 = \alpha_0 + 2\beta_1 + \theta_f - \pi/2$. Hence, using $\alpha_3 = \frac{\pi}{2} - \theta_f$

$$L_1 - L_2 = 2\pi + 2\gamma + 2\alpha_3 - 2\beta_1$$

and our aim is to prove that this quantity is positive. With the angles labelled as in Figure 3, noting that $\gamma = \pi - \bar{\gamma}$ and $\beta_1 = 2\pi - \phi$, we need to prove that $\bar{\gamma} < \phi + \alpha_3$. For this, defining $s := |c_3 - c_0|$ note that

$$|\tilde{c}_2 - c_0| = 8 - 8\cos\phi = 4 + s^2 - 2s\cos(\theta_0 - \alpha_3)$$

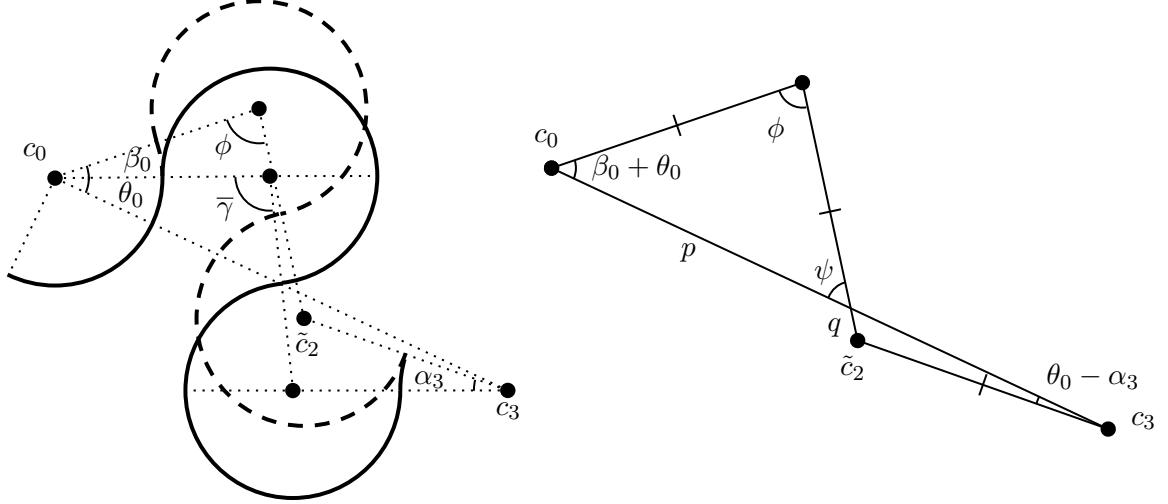


Figure 3: Left: trajectory of type $CCCC$ (solid) which satisfies the necessary conditions for optimality, and another of type CCC (dashed) which we prove is shorter, and can therefore be extended to a trajectory of type $CCSC$ (as in Figure 2) with the correct length. Right: enlargement of the internal triangles from the CCC trajectory.

and that this is still true if $\alpha_3 > \theta_0$. Supposing we allow α_3 to vary, then we determine that

$$\frac{d\phi}{d\beta_0} = -\frac{s \sin(\theta_0 - \alpha_3)}{4 \sin \phi} \frac{d\alpha_3}{d\beta_0}$$

Note that as β_0 increases so too does α_3 , and so $\frac{d\phi}{d\beta_0}$ is negative for $\alpha_3 < \theta_0$ and positive for $\alpha_3 > \theta_0$. It follows that

$$\frac{d}{d\beta_0}(\phi + \alpha_3) = \frac{d\phi}{d\beta_0} \left(1 - \frac{s \sin(\theta_0 - \alpha_3)}{4 \sin \phi} \right).$$

Since $\phi + \alpha_3 = \bar{\gamma}$ at $\beta_0 = 0$, if we can show that the above quantity is always positive then we have the required result: $\bar{\gamma} < \phi + \alpha_3$. When $\alpha_3 > \theta_0$ this is immediate: all the quantities on the right hand side are positive. For $\alpha_3 < \theta_0$ we refer to the right hand side of Figure 3 and observe that

$$\frac{\sin(\theta_0 - \alpha_3)}{q} = \frac{\sin \psi}{2} = \frac{\sin \phi}{p}$$

and therefore $\frac{\sin(\theta_0 - \alpha_3)}{\sin(\phi)} = \frac{q}{p}$. Now $\frac{d}{d\beta_0}(\phi + \alpha_3)$ will be positive if $4p > qs$. Comparing with Figure 3, we know $q < 1$ and since $\bar{\gamma} > \pi/2$ (by assumption) we have that $p > s/4$, so we are done with this case.

Case 1b: $\alpha_3 \geq \pi/2$ and $\gamma < \pi/2$. In this case we cannot reflect c_3 about θ_f . We set \tilde{c}_2 to $c_3 + 2i$ instead (i.e. vertically above c_3), and then construct a trajectory of type $CCSCC$. This is not very different to the previous case.

Case 2: $\gamma \geq \pi/2$. Referring to Figure 4, let $\tilde{w} := c_3 - \tilde{c}_1$ and then we have

$$\begin{aligned} \tilde{c}_1 &= 2e^{i\beta_0} \\ c_3 &= z_f + e^{i(\theta_f - \pi/2)} \\ l &= |\tilde{w}| \\ L_2 &= \alpha_0 + \beta_0 + \beta_1 + l + \beta_2 + \alpha_3 \\ &= \alpha_0 + 2\beta_0 + 2\pi + |\tilde{w}| + \alpha_3 \end{aligned}$$

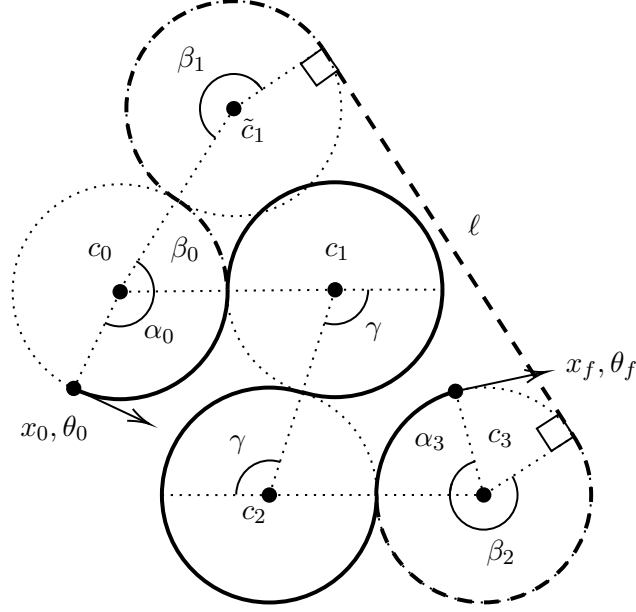


Figure 4: Diagram for Case 2 ($\gamma \geq \frac{\pi}{2}$) in the proof of Lemma 21: a trajectory of type $CCCC$ (solid) which satisfies the necessary conditions from the maximum principle, and another of type $CCSC$ (dashed) with the same maximum curvature which does not.

Arguing as in case 1, we have that L_2 depends continuously on β_0 and it is enough to show that $L_2 < L_1$ when $\beta_0 = 0$, where $L_1 = \alpha_0 + 2\pi + 2\gamma + \alpha_3$ is the length of the original trajectory. Indeed, at β_0 we have $L_1 - L_2 = 2\gamma - |\tilde{w}|$. Noting that $|\tilde{w}|^2 = 8 + 8 \cos \gamma$ and recalling that we have assumed $\gamma > \pi/2$ we have that $|\tilde{w}|^2 \leq 8 < (2\gamma)^2$ and therefore $L_1 > L_2$ at $\beta_0 = 0$. \square

Theorem 22 *Any solution to problem (P) is of type CXC or sub-path thereof, where X can be S , C , or O ; or of type SOS or sub-path thereof. The radii of all the C and O arcs in a solution are the same.*

Proof. First note that any path containing more than one loop cannot be optimal. The loops can be brought together without changing the maximum curvature, but a sub-path of type OO is not optimal - it can be expanded into a single loop with lower curvature. Consider all paths of type $SXYZ$, where X, Y, Z can each be C, O, S or void,

- $X = C$: SC can be optimal, SCY cannot, by Lemma 19.
- $X = O$: SO can be optimal and so can SOS , but SOO cannot by the argument above, and SOC is excluded by Lemma 20. Similarly, we rule out $SOSO$ and $SOSC$.
- A single straight line segment S can be optimal (similarly C and O).

By Lemma 18 we have exhausted the possibilities for optimal paths beginning with S . Next consider paths of type $CXYZ$:

- $X = C$: CC and CCC can be optimal, CCO and CCS are not optimal by Lemma 19. $CCCC$, $CCCO$ and $CCCS$ are excluded by Lemmas 21, Corollary 20 and Lemma 19 respectively.
- $X = O$: CO and COC can be optimal, COS is ruled out by Corollary 20 along with $COCC$ and $COCS$.

- $X = S$: CS and CSC are possible, CSO and $CSCO$ are not optimal by Corollary 20, and Lemma 19 rules out $CSCS$ and $CSCC$.

Finally, for paths of type $OXYZ$: OC can be optimal but OCC and OCS are not by Lemma 19 and Corollary 20 respectively, OS can be optimal but OSC is not by Lemma 20.

□

The boundary conditions that allow for paths of types SOS and COC are quite specific, and so we are able to prove a little more about the conditions under which these paths may be optimal.

Proposition 23 Consider an SOS path as per Figure 5, and let $d = \|z(0) - z(t_f)\|$ be the distance between the initial and final points. If $\frac{d}{t_f} > b$ where b is the solution of $\text{sinc}^{-1}(b)(1-b) = \pi/2$, then the path is not optimal.

Proof.

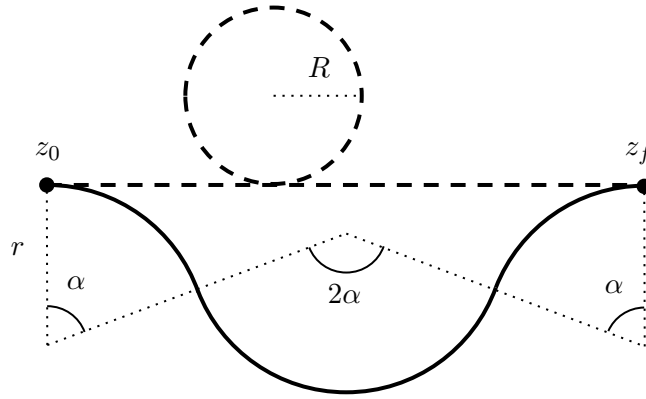


Figure 5: Diagram for the proof of Lemma 23: trajectory of type SCS , and a trajectory of type CCC with lower maximum curvature.

We show that with the assumption on d/t_f , the proposed trajectory of type CCC in Figure 5 has $r > R$. Note that $d = 4r \sin(\alpha)$ (still true if α is obtuse) and $t_f = 4r\alpha$ gives $d/t_f = \text{sinc}(\alpha)$. d/t_f is at most 1 and so $\text{sinc}^{-1}(d/t_f)$ has a solution between 0 and π and $\alpha = \text{sinc}^{-1}(d/t_f)$. Moreover from $2\pi R + d = t_f$ we then have

$$R = \frac{t_f - d}{2\pi} = \frac{4r(\alpha - \sin \alpha)}{2\pi}$$

and therefore $r > R$ while $2(\alpha - \sin \alpha)/\pi < 1$. Rewriting this inequality in terms of d/t_f gives

$$\text{sinc}^{-1}\left(\frac{d}{t_f}\right)\left(1 - \frac{d}{t_f}\right) < \frac{\pi}{2}$$

and on the domain $[0, 1)$ the left hand side of the inequality is decreasing.

□

Remark 24 Note that the full circular arc, or the loop, in Figure 5 can be placed anywhere on the straight line S without changing the maximum curvature or the boundary conditions and so the above result also applies to paths of type OS and SO . □

Note that a path of type COC cannot be optimal if the C 's have different orientations. If they do then the loop can be shifted to the terminal point to obtain a path of type CCO with the same maximum curvature, but such a path is not optimal by Lemma 19.

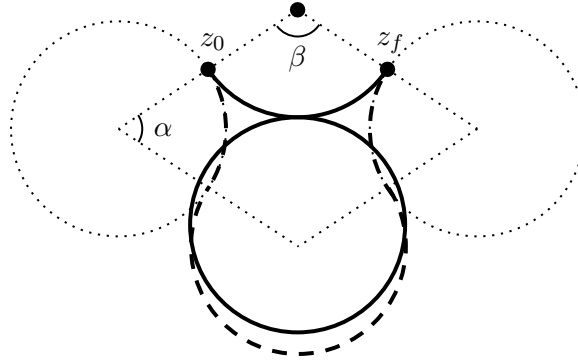


Figure 6: Diagram for Proposition 25: A path of type *COC* (solid) and shorter curve of type *CCC* (dashed) with the same maximum curvature.

Proposition 25 Consider a path of type *COC* and of length $t_f = \beta/a + 2\pi$ as in Figure 6 (solid). Such a path can be optimal only if $\beta \leq \frac{\pi}{2}$.

Proof. For comparison we consider the *CCC* path also pictured in Figure 6 (dashed). Assuming that the circular arcs all have radius 1, the length of the *COC* path is $L_1 = \beta + 2\pi$, and the length of the *CCC* is $L_2 = 2\alpha + 2\pi - \beta = 4\pi - 3\beta$. Therefore if $\beta > \frac{\pi}{2}$ then $L_2 < L_1$ and then, adjusting the angles as necessary, the radii of each of the circular arcs in the *CCC* curve can be increased (reducing the maximum curvature) until the curve has the correct length $\beta + 2\pi$, and so the original *COC* is not a minimiser. \square

Remark 26 Note that the full circular arc, or the loop, in Figure 6 can be placed anywhere on the circular arc C between z_0 and z_f without changing the maximum curvature or the boundary conditions and so the above result also applies to paths of type *OC* and *CO*. \square

The numerical experiments in Section 5.1, specifically Examples 1 and 2, suggest that the converses to Propositions 23 and 25 are true. It may be possible to verify this by direct comparison with each of the potential minimisers allowed by Theorem 22 which satisfy the constraints (at least in the *SOS* case there do not seem to be too many of these), but we will not attempt to do so here.

4.1 Proof of Proposition 2

Proof. The proof is sketched in [7] but for the convenience of the reader we fill out the details. For any $p \in [1, \infty)$, consider the p -elastic energy $\int_0^{t_f} \|\dot{z}(t)\|^p dt$ for z in the Sobolev space $W^{2,p}((0, t_f), \mathbb{R}^2)$ and satisfying the constraints of Problem (P). The existence of minimisers of the p -elastic energy subject to Dirichlet boundary conditions is proved using the direct method in [19, Proposition 4.1], and the same proof works for the boundary conditions we have here. We may therefore consider a sequence (z_p) where each z_p is a minimiser of the p -elastic energy subject to the constraints of problem (P), and let z_* be any element of $W^{2,\infty}((0, t_f), \mathbb{R}^2)$ satisfying the constraints. Then for any $p \geq q$, using the minimality of z_q and z_p and the embedding $L^p \subset L^q$ we have

$$\|\ddot{z}_q\|_{L^q} \leq \|\ddot{z}_p\|_{L^q} \leq c \|\ddot{z}_p\|_{L^p} \leq c \|\ddot{z}_*\|_{L^p} \leq t_f^{\frac{1}{q}} \|\ddot{z}_*\|_{L^\infty} \quad (21)$$

where $c = t_f^{\frac{1}{q} - \frac{1}{p}}$. Note also that for any $z \in W^{2,q}((0, t_f), \mathbb{R}^2)$ satisfying the constraints of (P), since $\|\dot{z}\| = 1$ we have $\|\dot{z}\|_{L^q} = t_f^{\frac{1}{q}}$, and if $q \geq 2$ then, using the fundamental theorem of calculus,

Cauchy-Schwarz' inequality and Young's inequality with ε :

$$\|z(t)\|^2 = \|z(0)\|^2 + \int_0^t \frac{d}{d\tau} \|z(\tau)\|^2 d\tau = \|z(0)\|^2 + \int_0^t \langle z(\tau), \dot{z}(\tau) \rangle d\tau \leq \|z(0)\|^2 + \frac{1}{2\varepsilon} \|z\|_{L^2}^2 + \frac{t\varepsilon}{2}.$$

Rearranging and integrating over $(0, t_f)$ gives

$$\|z\|_{L^2}^2 - \frac{t_f}{2\varepsilon} \|z\|_{L^2}^2 \leq t_f \|z(0)\|^2 + t_f^2 \varepsilon,$$

and then setting $\varepsilon = t_f$ gives

$$\|z\|_{L^q} \leq c \|z\|_{L^2}^2 \leq 2c(t_f \|z(0)\|^2 + t_f^3).$$

for $q \geq 2$. Combining these lower order estimates with (21), we have that for each $2 \leq q < \infty$ the subsequence $(z_p)_{p \geq q}$ is bounded in $W^{2,q}((0, t_f), \mathbb{R}^2)$, and therefore has a subsequence which converges weakly in $W^{2,q}((0, t_f), \mathbb{R}^2)$ (by the local weak compactness of reflexive Banach spaces, [23, p. 126]) and strongly in $C^1([0, t_f], \mathbb{R}^2)$ (by the Rellich-Kondrachov theorem, [1, Theorem 6.3]). By induction we can construct successive subsequences $(z_{p_2(i)}), (z_{p_3(i)}), \dots, (z_{p_k(i)}), \dots$, such that $(z_{p_{k+1}(i)})$ is a subsequence of $(z_{p_k(i)})$ which converges weakly in $W^{2,k+1}$. Then the diagonal sequence $(z_{\tilde{p}(i)})$ where $\tilde{p}(i) = p_i(i)$ converges weakly in $W^{2,k}$ for every $k \geq 2$. Indeed, since weak convergence in $W^{2,k}$ implies weak convergence in $W^{2,q}$ for all $q \leq k$ by the embedding $W^{2,q} \subset W^{2,k}$, we have that $z_{\tilde{p}(i)}$ converges weakly in $W^{2,q}$ (and strongly in C^1) for every $q \geq 2$ to $z_\infty \in \bigcap_{q \geq 2} W^{2,q}((0, t_f), \mathbb{R}^2)$. By the strong C^1 convergence, z_∞ satisfies the constraints. Since $\|\ddot{z}_\infty\|_{L^q}$ is uniformly bounded for all q , we have $z_\infty \in W^{2,\infty}((0, t_f), \mathbb{R}^2)$ and $\lim_{p \rightarrow \infty} \|\ddot{z}_\infty\|_{L^p} = \|\ddot{z}_\infty\|_{L^\infty}$ by [1, Theorem 2.14], and also $\lim_{p \rightarrow \infty} \|\ddot{z}_p\|_{L^p} = \|\ddot{z}_\infty\|_{L^\infty}$. Finally, z_∞ is a minimiser of maximum curvature, because if not then there exists z and $\varepsilon > 0$ such that $\|\ddot{z}\|_{L^\infty} = \|\ddot{z}_\infty\|_{L^\infty} - \varepsilon$, and then choosing p sufficiently large:

$$t_f^{-\frac{1}{p}} \|\ddot{z}_p\|_{L^p} > \|\ddot{z}_\infty\|_{L^\infty} - \frac{\varepsilon}{2} > \|\ddot{z}\|_{L^\infty} \geq t_f^{-\frac{1}{p}} \|\ddot{z}\|_{L^p}$$

which contradicts the assumption that z_p is a minimiser of the p -elastic energy. \square

5 A Numerical Method

In this section, we provide a numerical method utilizing *arc*, or *switching time*, *parametrization techniques* earlier used for optimal control problems exhibiting discontinuous controls in [12–14, 18]. Theorem 22 asserts that a curve of minimax curvature can be of type (described by the strings) *CCC*, or *COC*, or *CSC*, or *SOS*, or a substring thereof, and nothing else. Then the problem of finding such a curve can be reduced to finding a correct concatenation/configuration of circular arcs (*C*), straight lines (*S*) and a loop (*O*) as listed, as well as finding the length of each arc involved. Recall that a loop is nothing but a circular arc with length $2\pi/a$. Therefore, for computational purposes, we will treat a loop as any other circular arc *C* with an unknown length. We also note that if there are more than one circular arc in a string then they must have the same curvature a , i.e., the same radius.

A circular arc *C* can either be a left-turn or a right-turn arc, which we denote by *L* and *R*, respectively. Then a curve of type *CCC* can be represented by the string *LRLR*. Clearly, at least one of the arcs in *LRLR* must be of zero length in order to represent *CCC* or a substring thereof, and this should be determined by the numerical method to be proposed. A curve of type *CSC* can similarly be represented by *LRLSLR*, again with at least one of the arcs of type *L* or *R* being of zero length. Note that if the length of the straight line (*S*) is zero, then *LRLSLR* effectively reduces to *LRLR* representing *CCC*. Therefore, the string *LRLSLR* is general enough to represent both of the types *CCC* and *CSC*. The type *SCS* (or equivalently *SOS*), on the other hand, can be

represented by the string $SLRS$. Recall that, by Remark 24, any solution of type SOS can be obtained from a solution of type SO or OS , simply by placing the loop anywhere on the straight line segment between the endpoints. Therefore either the string SLR or the string LRS will suffice to represent SCS . As a result, one would cover all the solution types in Theorem 22 by using the string $LRSLLR$.

Let L_{ξ_1} denote a left-turn arc with length ξ_1 , R_{ξ_2} a right-turn arc with length ξ_2 and S_{ξ_3} a straight line with length ξ_3 . Similarly, let L_{ξ_4} denote a left-turn arc with length ξ_4 and R_{ξ_5} a right-turn arc with length ξ_5 . Then the types of solution curves described in Theorem 22 can all be represented by the string

$$L_{\xi_1}R_{\xi_2}S_{\xi_3}L_{\xi_4}R_{\xi_5}.$$

For example, the type $RLLR$ is given with $\xi_1 = \xi_3 = 0$ and $\xi_2, \xi_4, \xi_5 > 0$. On the other hand, the type LR is obtained either with $\xi_3 = \xi_4 = \xi_5 = 0$ and $\xi_1, \xi_2 > 0$ or with $\xi_1 = \xi_2 = \xi_3 = 0$ and $\xi_4, \xi_5 > 0$.

Let the initial time $t_0 := 0$ and the terminal time $t_5 := t_f$. Also define the *switching times* t_j , $j = 1, \dots, 4$, such that

$$\xi_j := t_j - t_{j-1}, \quad \text{for } j = 1, \dots, 5. \quad (22)$$

The lengths ξ_j may also be referred to as *arc durations*. Note that along an arc of type L or R the optimal control is bang–bang; in particular, $v(t) \equiv 1$ along an arc of type L and $v(t) \equiv -1$ along an arc of type R . Along an arc of type S , on the other hand, optimal control is singular; in particular, $v(t) \equiv 0$, by Lemma 7. Since $v(t)$ is constant (1, -1 or 0) for $t_{j-1} \leq t < t_j$ (along the j th arc), the ODEs in Problem (OC) with $\alpha(t) = a$, or equivalently Problem (Pc) with $u(t) = a v(t)$, can be solved as follows.

$$\theta(t) = \theta(t_{j-1}) + a v(t) (t - t_{j-1}), \quad \text{if } j = 1, \dots, 5, \quad (23)$$

$$x(t) = \begin{cases} x(t_{j-1}) + (\sin \theta(t) - \sin \theta(t_{j-1})) / (a v(t)), & \text{if } j = 1, 2, 4, 5, \\ x(t_{j-1}) + \cos \theta(t) (t - t_{j-1}), & \text{if } j = 3, \end{cases} \quad (24)$$

$$y(t) = \begin{cases} y(t_{j-1}) + (\cos \theta(t) - \cos \theta(t_{j-1})) / (a v(t)), & \text{if } j = 1, 2, 4, 5, \\ y(t_{j-1}) + \sin \theta(t) (t - t_{j-1}), & \text{if } j = 3, \end{cases} \quad (25)$$

where

$$v(t) = \begin{cases} 1, & \text{if } j = 1, 4, \\ -1, & \text{if } j = 2, 5, \\ 0, & \text{if } j = 3, \end{cases} \quad (26)$$

for $t_{j-1} \leq t < t_j$. We have used the solution for $\theta(t)$ in (23) in obtaining the solutions for $x(t)$ and $y(t)$ in (24)–(25). Note that the control variable $v(t)$ is a piecewise constant function, which takes here the sequence of values $\{1, -1, 0, 1, -1\}$. It should be clear from the context that the control variable $u(t)$ defined in Problem (Pc) takes the sequence of values $\{a, -a, 0, a, -a\}$. After evaluating the state variables in (23)–(25) at the switching times and carrying out algebraic manipulations,

one can equivalently rewrite Problem (Pc), or Problem (OC), as follows.

$$(Ps) \left\{ \begin{array}{l} \min \quad a \\ \text{s.t.} \quad x_0 - x_f + \frac{1}{a}(-\sin \theta_0 + 2 \sin \theta_1 - 2 \sin \theta_2 + 2 \sin \theta_4 - \sin \theta_f) + \xi_3 \cos \theta_2 = 0, \\ \quad y_0 - y_f + \frac{1}{a}(\cos \theta_0 - 2 \cos \theta_1 + 2 \cos \theta_2 - 2 \cos \theta_4 + \cos \theta_f) + \xi_3 \sin \theta_2 = 0, \\ \quad \sin \theta_f = \sin \theta_5, \quad \cos \theta_f = \cos \theta_5, \\ \quad t_f = \sum_{j=1}^5 \xi_j, \quad \xi_j \geq 0, \quad \text{for } j = 1, \dots, 5, \end{array} \right.$$

where

$$\theta_1 = \theta_0 + a \xi_1, \quad \theta_2 = \theta_1 - a \xi_2, \quad \theta_4 = \theta_2 + a \xi_4, \quad \theta_5 = \theta_4 - a \xi_5. \quad (27)$$

Substitution of θ_1 , θ_2 , θ_4 and θ_5 in (27) into Problem (Ps) yields a finite-dimensional nonlinear optimization problem in just six variables, ξ_j , $j = 1, \dots, 5$, and a .

Remark 27 With the constraints $\sin \theta_f = \sin \theta_5$ and $\cos \theta_f = \cos \theta_5$, we make sure that we satisfy the slope condition at the terminal point. Otherwise, the constraint $\theta_f = \theta_5$ is stronger, and imposing it might result in missing some of the feasible solutions. \square

Remark 28 Problem (Ps) can be solved by standard optimization methods and software, for example, Algencon [2, 3], which implements augmented Lagrangian techniques, or Ipopt [22], which implements an interior point method, or SNOPT [8], which implements a sequential quadratic programming algorithm, or Knitro [4], which implements various interior point and active set algorithms to choose from. For general nonconvex optimization problems like Problem (Ps), what one can hope for, by using these software, is to get (at best) a locally optimal solution. \square

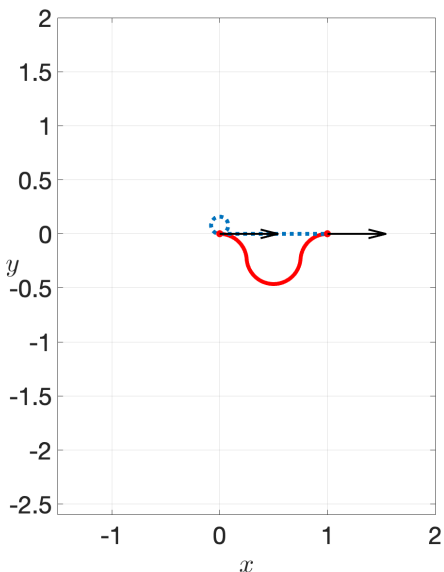
5.1 Numerical experiments

For computations numerically solving Problem (Ps), or equivalently Problem (P), we have employed the AMPL–Knitro computational suite: AMPL is an optimization modelling language [6] and Knitro is a popular optimization software [4] (Version 3.0.1 is used here). In all runs, we have used the Knitro options ‘alg=0 feastol=1e-12 opttol=1e-12’ in AMPL; in other words, we have set both the feasibility and optimality tolerances at 10^{-12} , and the particular algorithm to be employed was left to be chosen by Knitro itself.

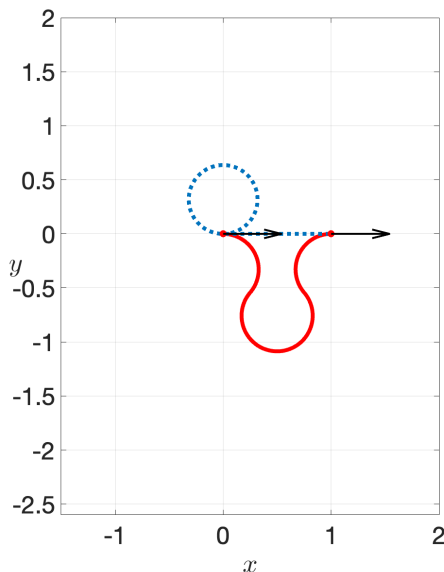
In what follows, we present example instances of problems for which we solve Problem (Ps) by using the AMPL–Knitro suite and display the solution curves. The best numerical solution we have identified for an instance is depicted by a solid curve in the graphs. The other solutions reported by the suite as “locally optimal” are depicted by dotted curves, and referred to here as “critical”, as they satisfy the necessary conditions of optimality furnished by the maximum principle.

5.1.1 Example 1

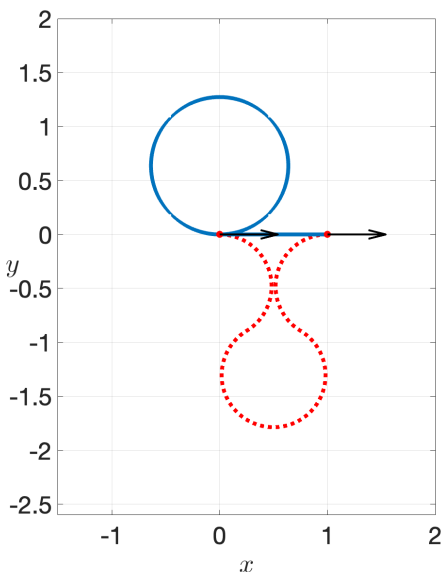
Recall from Corollary 23 that b is the solution of the equation $\text{sinc}^{-1}(b)(1-b) = \pi/2$. After rearranging this equation one gets $f(b) := b - \text{sinc}(\pi/(2(1-b))) = 0$. A numerical solution to $f(b) = 0$ can be obtained as $b \approx 0.319966693534110$ (correct to 15 dp) in seven iterations by using the secant method starting with initial points 0.1 and 0.2. The uniqueness of this solution can be established by observing that the graph of f crosses the b -axis only once (not shown here).



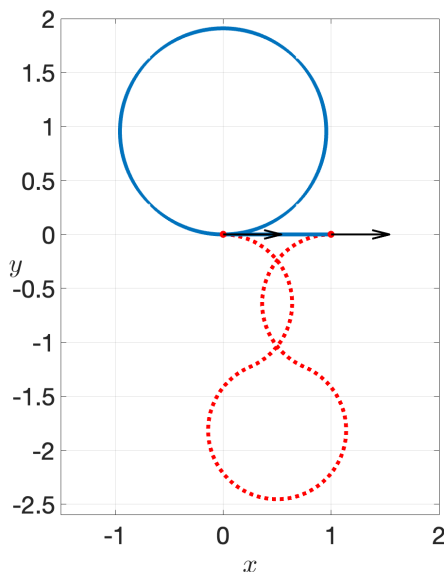
(a) $t_f = 1.5$: Solid curve RLR (red) with $a \approx 3.989$; dotted curve LS (blue) with $a = 4\pi$.



(b) $t_f = 3$: Solid curve RLR (red) with $a \approx 3.038$; dotted curve LS (blue) with $a = \pi$.



(c) $t_f = 5$: Solid curve LS (blue) with $a = \pi/2$; dotted curve RLR (red) with $a \approx 2.077$.



(d) $t_f = 7$: Solid curve LS (blue) with $a = \pi/3$; dotted curve RLR (red) with $a \approx 1.565$.

Figure 7: Example 1—Problem instances for Proposition 23 and its converse: (a)–(b) for $d/t_f > b$ ($t_f \leq 3.12532$) and (c)–(d) for $d/t_f \leq b$ ($t_f \geq 3.12533$)—Curves of minimax curvature between the oriented points $(0, 0, 0)$ and $(0, 1, 0)$, for various t_f . The solid curves are optimal (identified by numerical experiments) while the dotted ones are only critical.

Figure 7 shows curves of minimax curvature between the oriented points $(x_0, y_0, \theta_0) = (0, 0, 0)$ and $(x_f, y_f, \theta_f) = (0, 1, 0)$, which is a similar situation to that in the diagram in Figure 5. The orientation of the endpoints of the curves in Figure 7 are depicted by (black) arrows. We note that, for the two given endpoints, $d = 1$.

Proposition 23 asserts that the *SOS* type of trajectory is not optimal (nor *OS* or *SO*, by Remark 24) for $t_f < 1/b$, i.e., $t_f \leq 3.12532$ (correct to 5 dp). This is exemplified in Figures 7(a)

and 7(b) respectively for $t_f = 1.5$ and $t_f = 3$, where it is numerically verified that the CCC concatenation of curves is optimal: For $t_f = 1.5$, the solution curve has $a = 3.9887508486$ (correct to 10 dp) and is of type $R_{\xi_2}L_{\xi_4}R_{\xi_5}$ (with $\xi_1 = \xi_3 = 0$), where the arc lengths $\xi_2 = 0.375$, $\xi_4 = 0.75$, and $\xi_5 = 0.375$. For $t_f = 3$, $a = 3.0384835468$ (correct to 10 dp) and the solution is of the same type, with $\xi_2 = 0.75$, $\xi_4 = 1.5$, and $\xi_5 = 0.75$. We point to the symmetry in the arc lengths in both cases, presumably because of the colinear configuration of the endpoints.

The converse of Proposition 23 for this example instance (which is not proved) is that the *SOS* (or *OS* or *SO*, by Remark 24) concatenation is optimal for $t_f \geq 1/b$, i.e., $t_f \geq 3.12533$ (correct to 5 dp). This converse is exemplified in Figures 7(c) and 7(d) respectively for $t_f = 5$ and $t_f = 7$. For $t_f = 5$, the solution curve has $a = \pi/2$ and is of type $L_{\xi_1}S_{\xi_3}$ (with $\xi_2 = \xi_4 = \xi_5 = 0$), where $\xi_1 = 4$, and $\xi_3 = 1$. For $t_f = 7$, $a = \pi/3$ and the solution is of the same type, with $\xi_1 = 6$, and $\xi_3 = 1$.

Each of the solution curves presented in Figure 7 can be “flipped over” or “reflected about” the x -axis to get “symmetric” solution curves: For example when an *LS* curve is reflected one gets an *RS* curve which has the same length, oriented endpoints and maximum curvature. An *RLR* curve can also be reflected in the same way to get an *LRL* curve which has the same length, oriented endpoints and maximum curvature. These reflected curves have also been obtained as computational solutions to Problem (Ps).

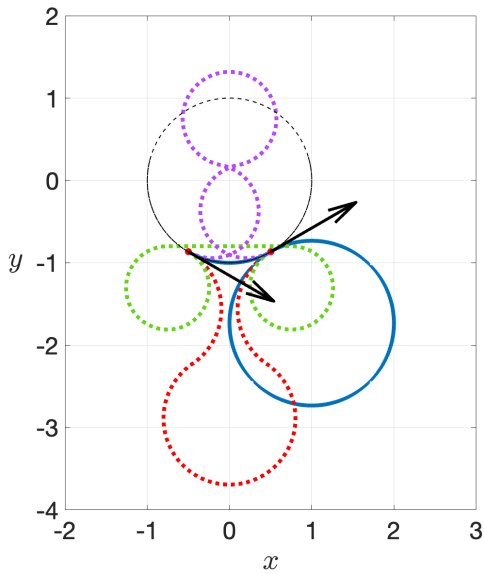
5.1.2 Example 2

Suppose that the endpoints are placed on a unit circle with the end velocities chosen tangent to the circle. Recall from Proposition 25 that a curve of minimax curvature between these endpoints can be of type *COC* (or equivalently type *OC* or type *CO*, as the loop O can be shifted anywhere on a circular arc C) only in the case when the endpoints are separated by at most $\pi/2$ radians, i.e., they are separated by an angle $\beta \leq \pi/2$ (see Figure 6), and t_f is chosen as $\beta + 2\pi$. Here we numerically illustrate Proposition 25 and explore instances with various other values of the separation angle β and with $t_f = \beta + 2\pi$ —see Figure 8(a)–(d).

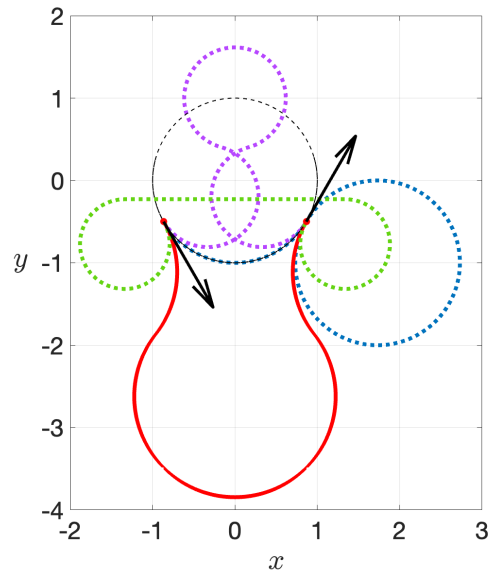
We place the pair of oriented endpoints on a unit circle, and impose $t_f = \beta + 2\pi$ (so that a loop can be observed at least in a critical curve), in each part of Figure 8, and obtain optimal solutions as follows.

- (a) $\beta = \pi/3 < \pi/2$, i.e., $t_f = 7\pi/3$: $(-1/2, -\sqrt{3}/2, -\pi/6)$ and $(1/2, -\sqrt{3}/2, \pi/6)$. The optimal curve is of type $L_{\xi_4}R_{\xi_5}$ (with $\xi_1 = \xi_2 = \xi_3 = 0$), where $a = 1$, $\xi_4 = \pi/3$, and $\xi_5 = 2\pi$.
- (b) $\beta = 2\pi/3$, i.e., $t_f = 8\pi/3$: $(-\sqrt{3}/2, -1/2, -\pi/3)$ and $(\sqrt{3}/2, -1/2, \pi/3)$. The optimal curve is of type $R_{\xi_2}L_{\xi_4}R_{\xi_5}$ (with $\xi_1 = \xi_3 = 0$), where $a = 0.8174619979$, $\xi_2 = 1.4538775285$, $\xi_4 = 5.4698253525$, and $\xi_5 = 1.4538775285$, all correct to 10 dp.
- (c) $\beta = 4\pi/3$, i.e., $t_f = 10\pi/3$: $(-\sqrt{3}/2, 1/2, -2\pi/3)$ and $(\sqrt{3}/2, 1/2, 2\pi/3)$. The optimal curve is of type $R_{\xi_2}L_{\xi_4}R_{\xi_5}$, where $a = 0.5245840019$, $\xi_2 = 0.6217500975$, $\xi_4 = 9.2284753170$, and $\xi_5 = 0.6217500975$, all correct to 10 dp.
- (d) $\beta = 5\pi/3$, i.e., $t_f = 11\pi/3$: $(-1/2, \sqrt{3}/2, -5\pi/6)$ and $(1/2, \sqrt{3}/2, 5\pi/6)$. The optimal curve is of type $R_{\xi_2}L_{\xi_4}R_{\xi_5}$, where $a = 0.5026360614$, $\xi_2 = 0.2755293870$, $\xi_4 = 10.9681142892$, and $\xi_5 = 0.2755293870$, all correct to 10 dp.

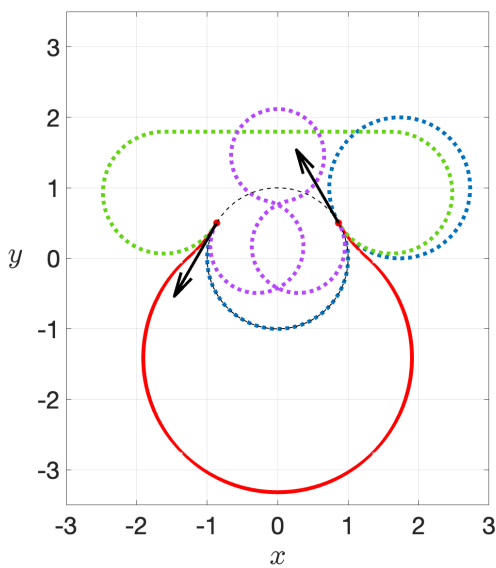
In each of the problem instances, one curve of *CO* type, two curves of *CCC* type, and one curve of *CSC* type have been found as solutions of Problem (Ps) by the AMPL–Knitro suite. Of these four distinct solutions in each case, the curve with the smallest a was identified as the optimal curve for that case.



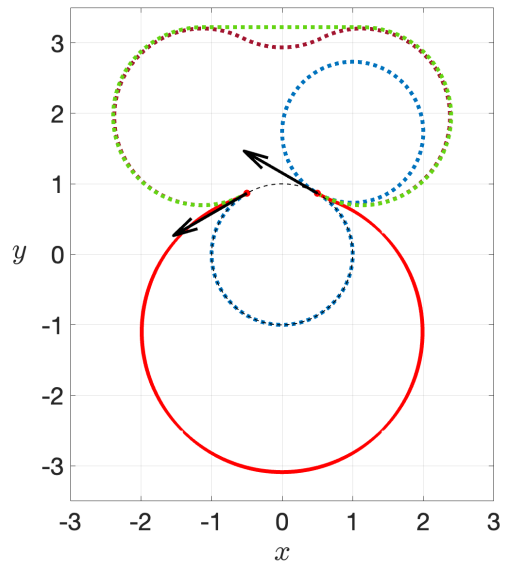
(a) $\beta = \pi/3$: Solid curve LR (blue) with $a = 1$; dotted curves, RLR (red) with $a \approx 1.246$, LRL (purple) with $a \approx 1.754$, RSR (green) with $a \approx 1.978$.



(b) $\beta = 2\pi/3$: Solid curve RLR (red) with $a \approx 0.817$; dotted curves, LR (blue) with $a = 1$, LRL (purple) with $a \approx 1.620$, RSR (green) with $a \approx 1.836$.



(c) $\beta = 4\pi/3$: Solid curve RLR (red) with $a \approx 0.525$; dotted curves, LR (blue) with $a = 1$, RSR (green) with $a \approx 1.157$, LRL (purple) with $a \approx 1.514$.



(d) $\beta = 5\pi/3$: Solid curve RLR (red) with $a \approx 0.503$; dotted curves, RSR (green) with $a \approx 0.792$, RLR (brown) with $a \approx 0.798$, LR (blue) with $a = 1$.

Figure 8: Example 2—Problem instances for Corollary 25: Curves of minimax curvature (and of particular length) between oriented points placed on a unit circle. The solid curves are optimal (identified by numerical experiments) while the dotted ones are only critical.

Similarly to Example 5.1.1, the loop in each of the LR curves presented in Figure 8 can be “flipped over” or “reflected about” the circle to get “symmetric” curves of type L with $\xi_1 = \beta + 2\pi$, with the same endpoints and maximum curvatures. These reflected curves have also been encountered as computational solutions to Problem (Ps), but are not being shown in Figure 8.

We note that if $t_f \neq \beta + \pi/2$ then one does not encounter a solution curve (optimal or only critical) which contains a loop.

5.1.3 Example 3

Consider the problem of finding a curve of minimax curvature between the oriented points $(0, 0, -\pi/3)$ and $(0.4, 0.4, -\pi/6)$ —note that the same oriented endpoints were used in [10] for finding the shortest curve of bounded curvature, i.e., the Markov–Dubins path. For various lengths, namely for $t_f = 0.8, 1.3, 2$ and 2.5 , here we find curves minimizing the bound a on the curvature. Figure 9(a)–(d) depict these curves found as a solution of Problem (Ps) by employing the AMPL–Knitro software suite.

In Figure 9(a)–(d), the optimal curves are shown as solid curves. These curves have been identified amongst all the critical solutions to Problem (Ps) (of the allowed types) that the AMPL–Knitro suite could find, as the ones with the smallest curvature, or indeed with the biggest turning radius. All other critical curves are shown as dotted curves in Figure 9(a)–(d). A summary of all these solutions in each part of Figure 9 can be given as follows, with arc lengths and curvatures correct up to 10 dp.

- (a) $t_f = 0.8$: The optimal curve has $a = 8.3661513485$ and is of type $L_{\xi_1}S_{\xi_3}R_{\xi_5}$ (with $\xi_2 = \xi_4 = 0$), where $\xi_1 = 0.3141136578$, $\xi_3 = 0.2343580660$, $\xi_5 = 0.2515282761$. Only one other critical curve is found which has $a = 24.6216106492$ and is of type RSR .
- (b) $t_f = 1.3$: The optimal curve has $a = 6.0477371511$ and is of type $R_{\xi_2}L_{\xi_4}R_{\xi_5}$ with $\xi_2 = 0.0684530840$, $\xi_4 = 0.6932888171$, $\xi_5 = 0.5382580988$. Four other critical curves are found which respectively have $a = 7.8842574114$, $a = 15.7179879207$, $a = 9.3041564227$, $a = 6.4570352671$, and are of types RSR , RSL , LSL , LRL .
- (c) $t_f = 2$: The optimal curve has $a = 4.0557744873$ and is of type $R_{\xi_2}S_{\xi_3}R_{\xi_5}$ with $\xi_2 = 1.1520596173$, $\xi_3 = 0.5799046398$, $\xi_5 = 0.2680357429$. Five other critical curves are found which respectively have $a = 8.1329787696$, $a = 4.1795061273$, $a = 4.7799043550$, $a = 4.9575871447$, $a = 5.0128303633$ and are of types RSL , RLR , LSL , LRL , LRL .
- (d) $t_f = 2.5$: The optimal curve has $a = 3.0172721767$ and is of type $R_{\xi_2}S_{\xi_3}R_{\xi_5}$ with $\xi_2 = 1.5726285431$, $\xi_3 = 0.5911279480$, $\xi_5 = 0.3362435090$. Six other critical curves are found which respectively have $a = 6.0662510507$, $a = 3.0516505811$, $a = 3.8632611845$, $a = 3.5528730863$, $a = 4.1925834507$, $a = 3.6102865904$ and are of types RSL , RLR , RLR , LSL , LRL , LRL .

6 Conclusion

We have presented a classification of the solutions to the problem of finding planar curves of minimax curvature between two endpoints with the endpoint tangents specified (Problem (P)). We devised a numerical procedure for finding the critical points of Problem (P), or the ∞ -elastica, of the classification types we have presented. Of these critical solutions the one with the smallest curvature is the (global) solution to Problem (P), which we refer to as a curve of minimax curvature.

A natural extension of this paper would be the study of interpolating curves which not only satisfy the endpoint constraints but also must pass through a number of specified intermediate points.

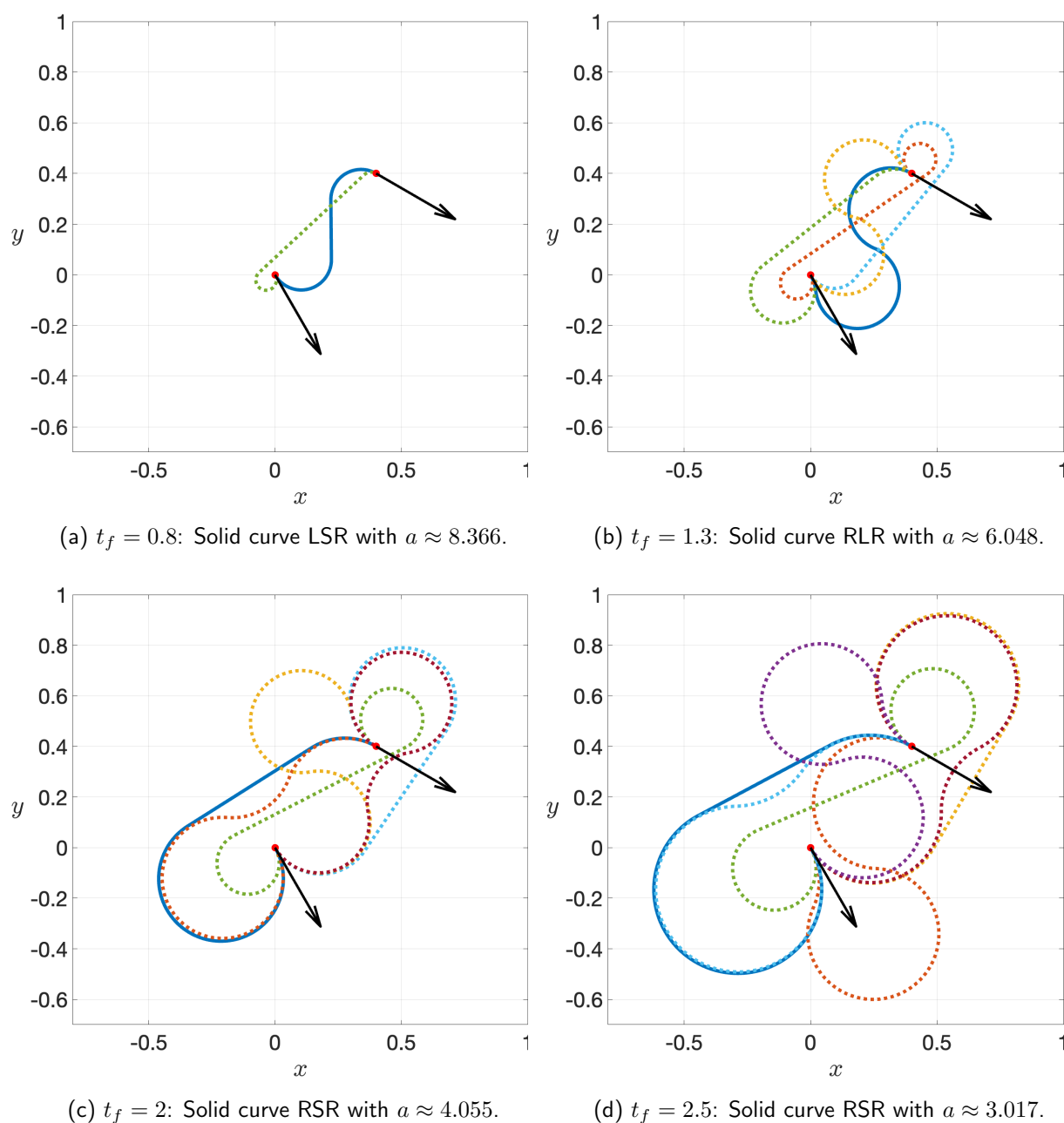


Figure 9: Example 3—Curves of minimax curvature between the oriented points $(0, 0, -\pi/3)$ and $(0.4, 0.4, -\pi/6)$. The solid (blue) curves are optimal (identified by numerical experiments) while the dotted ones (in various other colours) are only critical.

It would also be interesting to study another extension of Problem (P), from curves in \mathbb{R}^2 to curves in \mathbb{R}^n . In \mathbb{R}^3 alone, it is highly likely that one would encounter curve segments of types different from just circular and straight line segments.

A further extension from the Euclidean space to curved spaces would be of great interest where the curves of minimax curvature would be in a Riemannian manifold.

References

- [1] R. A. ADAMS, J. J. F. FOURNIER, *Sobolev Spaces*, Second Edition, Elsevier, 2003.

- [2] R. ANDREANI, E. G. BIRGIN, J. M. MARTÍNEZ, AND M. L. SCHUVERDT, *On augmented Lagrangian methods with general lower-level constraints*, SIAM J. Optim., 18(4) (2008), pp. 1286–1309.
- [3] E. G. BIRGIN AND J. M. MARTÍNEZ, *Practical Augmented Lagrangian Methods for Constrained Optimization*, SIAM Publications, 2014.
- [4] R. H. BYRD, J. NOCEDAL, R. A. WALTZ, *KNITRO: An integrated package for nonlinear optimization*. In: G. di Pillo and M. Roma, eds., Large-Scale Nonlinear Optimization, Springer, New York, 35–59, 2006. https://doi.org/10.1007/0-387-30065-1_4
- [5] L. E. DUBINS, *On curves of minimal length with a constraint on average curvature and with prescribed initial and terminal positions and tangents*, Amer. J. Math., 79 (1957), pp. 497–516.
- [6] R. FOURER, D. M. GAY, AND B. W. KERNIGHAN, *AMPL: A Modeling Language for Mathematical Programming, Second Edition*, Brooks/Cole Publishing Company / Cengage Learning, 2003.
- [7] E. GALLAGHER AND R. MOSER, *The ∞ -elastica problem on a Riemannian manifold*, J. Geom. Anal., 33(7) (2023), 226.
- [8] P. E. GILL, W. MURRAY, AND M. A. SAUNDERS, *SNOPT: an SQP algorithm for large-scale constrained optimization*, SIAM Rev., 47(1) (2005), 99–131.
- [9] R. HUANG, *A note on the p -elastica in a constant sectional curvature manifold*, J. Geom. Phys., 49(3–4) (2004), 343–349.
- [10] C. Y. KAYA, *Markov–Dubins path via optimal control theory*, Comput. Optim. Appl., 68(3) (2017), 719–747.
- [11] C. Y. KAYA, *Markov–Dubins interpolating curves*, Comput. Optim. Appl., 73(2) (2019), 647–677.
- [12] C. Y. KAYA, S. K. LUCAS, AND S. T. SIMAKOV, *Computations for bang–bang constrained optimal control using a mathematical programming formulation*, Opt. Contr. Appl. Meth., 25 (2004), 295–308.
- [13] C. Y. KAYA AND J. L. NOAKES, *Computations and time-optimal controls*, Opt. Contr. Appl. Meth., 17 (1996), 171–185.
- [14] C. Y. KAYA AND J. L. NOAKES, *Computational algorithm for time-optimal switching control*, J. Optim. Theory Appl., 117 (2003), 69–92.
- [15] C. Y. KAYA AND J. L. NOAKES, *Finding interpolating curves minimizing L^∞ acceleration in the Euclidean space via optimal control theory*, SIAM J. Control Optim., 51(1) (2013), 442–464.
- [16] M. G. KREĬN AND A. A. NUDEL’MAN, *The Markov Moment Problem and Extremal Problems*, Translations of Mathematical Monographs, Amer. Math. Soc., 1977.
- [17] A. A. MARKOV, *Some examples of the solution of a special kind of problem on greatest and least quantities*, Soobschenija Charkovskogo Matematicheskogo Obschestva, 2-1(5,6), 250–276, 1889 (in Russian).
- [18] H. MAURER, C. BÜSKENS, J.-H. R. KIM, AND C. Y. KAYA, *Optimization methods for the verification of second order sufficient conditions for bang–bang controls*, Opt. Contr. Appl. Meth., 26 (2005), 129–156.
- [19] T. MIURA AND K. YOSHIZAWA, *Pinned planar p -elasticae*, arXiv preprint [arXiv:2209.05721](https://arxiv.org/abs/2209.05721) (2022).
- [20] R. MOSER, *Structure and classification results for the ∞ -elastica problem*, Amer. J. Math., 144(5) (2022), 1299–1329.
- [21] L. S. PONTRYAGIN, V. G. BOLTYANSKII, R. V. GAMKRELIDZE, AND E. F. MISHCHENKO, *The Mathematical Theory of Optimal Processes* (Russian), English translation by K. N. Trivogoff, ed. by L. W. Neustadt, Interscience Publishers, New York, 1962.
- [22] A. WÄCHTER AND L. T. BIEGLER, *On the implementation of a primal-dual interior point filter line search algorithm for large-scale nonlinear programming*, Math. Program., 106 (2006), 25–57.
- [23] K. YOSIDA, *Functional Analysis*, Fifth Edition, Springer-Verlag, 1978.